Small Molecule Therapeutics

Molecular Cancer Therapeutics

Antitumor Activity of the Glutaminase Inhibitor CB-839 in Triple-Negative Breast Cancer

Matt I. Gross[1], Susan D. Demo[1], Jennifer B. Dennison[2], Lijing Chen[1], Tania Chernov-Rogan[1], Bindu Goyal[1], Julie R. Janes[1], Guy J. Laidig[1], Evan R. Lewis[1], Jim Li[1], Andrew L. MacKinnon[1], Francesco Parlati[1], Mirna L.M. Rodriguez[1], Peter J. Shwonek[1], Eric B. Sjogren[1], Timothy F. Stanton[1], Taotao Wang[1], Jinfu Yang[1], Frances Zhao[1], and Mark K. Bennett[1]

Abstract

Glutamine serves as an important source of energy and building blocks for many tumor cells. The first step in glutamine utilization is its conversion to glutamate by the mitochondrial enzyme glutaminase. CB-839 is a potent, selective, and orally bioavailable inhibitor of both splice variants of glutaminase (*KGA* and *GAC*). CB-839 had antiproliferative activity in a triple-negative breast cancer (TNBC) cell line, HCC-1806, that was associated with a marked decrease in glutamine consumption, glutamate production, oxygen consumption, and the steady-state levels of glutathione and several tricarboxylic acid cycle intermediates. In contrast, no antiproliferative activity was observed in an estrogen receptor–positive cell line, T47D, and only modest effects on glutamine consumption and downstream metabolites were observed. Across a panel of breast cancer cell lines, GAC protein expression and glutaminase activity were elevated in the majority of TNBC cell lines relative to receptor positive cells. Furthermore, the TNBC subtype displayed the greatest sensitivity to CB-839 treatment and this sensitivity was correlated with (i) dependence on extracellular glutamine for growth, (ii) intracellular glutamate and glutamine levels, and (iii) *GAC* (but not *KGA*) expression, a potential biomarker for sensitivity. CB-839 displayed significant antitumor activity in two xenograft models: as a single agent in a patient-derived TNBC model and in a basal like HER2$^+$ cell line model, JIMT-1, both as a single agent and in combination with paclitaxel. Together, these data provide a strong rationale for the clinical investigation of CB-839 as a targeted therapeutic in patients with TNBC and other glutamine-dependent tumors. *Mol Cancer Ther; 13(4); 890–901. ©2014 AACR.*

Introduction

Tumor cells use a variety of oncogenically- and environmentally driven metabolic pathways to meet the bioenergetic and biosynthetic demands of rapid and sustained growth (1, 2). One of the key nutrients that fuels the growth of many cancers is the amino acid glutamine, the most abundant amino acid in plasma (3, 4). A critical step in the utilization of glutamine is its conversion to glutamate by the mitochondrial enzyme glutaminase (5, 6). Glutamate and glutamate-derived metabolites in turn support a number of crucial cellular pathways including the tricarboxylic acid (TCA) cycle, redox balance, and amino acid synthesis.

Suppression of the broadly expressed form of glutaminase (encoded by the gene *GLS*) with either small-molecule inhibitors or by genetic knockdown has antitumor activity across a variety of tumor types, including lymphoma, glioma, breast, pancreatic, non–small cell lung and renal cancers (6–14). In addition, elevated *GLS* expression is associated with high grade and metastatic breast cancer (15). In particular, triple-negative breast cancer (TNBC) primary tumors and cell lines have elevated *GLS* mRNA; this is associated with high glutamine consumption and/or enhanced reliance on exogenous glutamine for survival *in vitro* (14, 16). Together, these observations highlight the critical connection between tumor growth and glutamine utilization and suggest that glutaminase inhibitors may provide therapeutic benefit in the treatment of a variety of cancers, including TNBC.

Several small-molecule inhibitors of glutaminase have been reported (6, 17–19). Glutamine analogs, 6-diazo-5-oxo-L-norleucine, azaserine and acivicin, bind irreversibly to the active site of a number of glutamine-utilizing enzymes, including glutaminase (20). Clinical studies with these compounds showed limited antitumor activity but their development was restricted by severe toxicities,

Authors' Affiliations: [1]Calithera Biosciences, South San Francisco, California; and [2]Department of Systems Biology, The University of Texas MD Anderson Cancer Center, Houston, Texas

Note: Supplementary data for this article are available at Molecular Cancer Therapeutics Online (http://mct.aacrjournals.org/).

M. Gross and S. Demo contributed equally to this work.

Corresponding Author: Mark K. Bennett, Calithera Biosciences, 343 Oyster Point Boulevard, Suite 200, South San Francisco, CA 94080. Phone: 650-870-1020; Fax: 650-588-5272; E-mail: mbennett@calithera.com

doi: 10.1158/1535-7163.MCT-13-0870

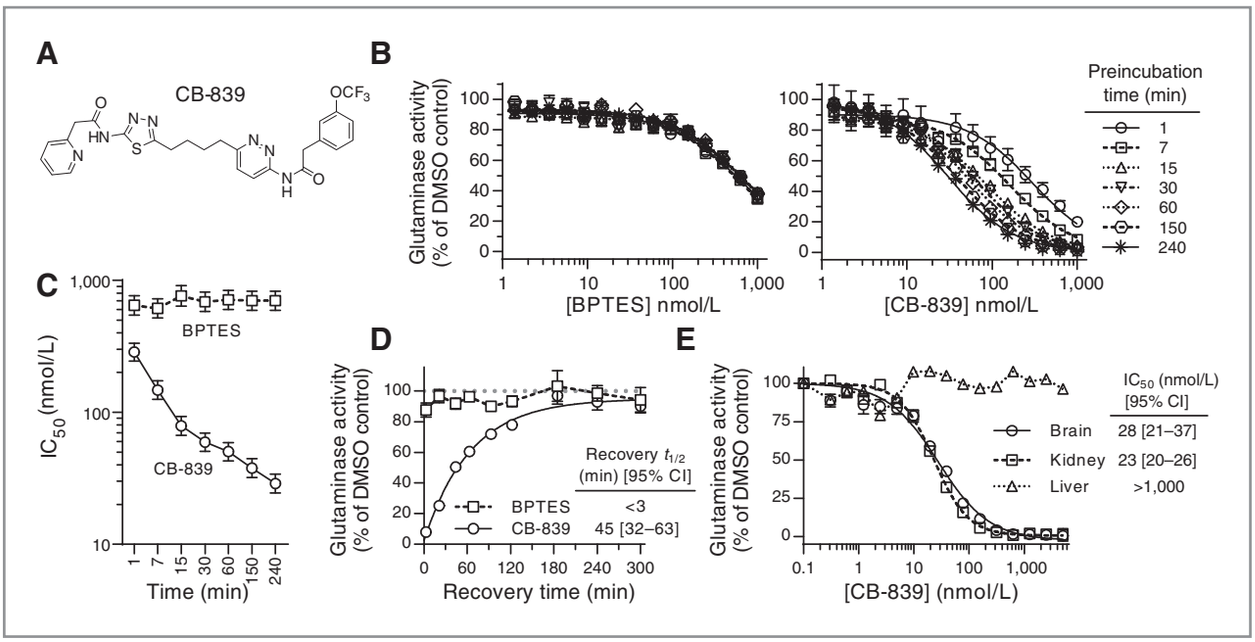

Figure 1. CB-839 potently inhibits glutaminase with time-dependent and slowly reversible kinetics. A, structure of CB-839. B, dose–response curves for BPTES (left) and CB-839 (right) following preincubation with rHu-GAC for the indicated times. C, time dependence of BPTES and CB-839 potency determined from the dose–response curves in B; IC_{50} and 95% confidence intervals (CI) are plotted. D, recovery of glutaminase activity after removal of BPTES or CB-839 from rHu-GAC by gel filtration. E, dose–response curves and IC_{50} determinations for endogenous glutaminase in kidney, brain, and liver homogenates treated with CB-839 for 1 hour. For B, D, and E, the percent activity relative to untreated controls (mean and SEM of at least duplicate measurements) are plotted. Results are representative of at least two independent experiments. Nonlinear curve fits (4 parameter dose response for B and E, one phase association for D) were used to calculate IC_{50} values, recovery $t_{1/2}$, and associated 95% CI values.

potentially due to the broad antagonism of multiple glutamine-utilizing enzymes and transporters (17). More recently, two allosteric inhibitors of glutaminase have been reported, compound 968 and BPTES (bis-2-(5-phenylacetamido-1,2,4-thiadiazol-2-yl)ethyl sulfide), that act by distinct mechanisms (6, 18, 21). The allosteric mechanism for BPTES (and BPTES analogs) entails formation of an inactive glutaminase homotetramer through the binding of two inhibitor molecules at the interface between a pair of homodimers (18, 22, 23). Several groups have reported antitumor activity for BPTES in lymphoma, breast, glioma, pancreatic, lung, and renal tumor types (7, 9, 11–13, 24). However, the moderate potency, poor metabolic stability, and low solubility of BPTES limit its potential for clinical development.

We report here the discovery and characterization of CB-839, a potent and selective inhibitor of glutaminase. CB-839 exhibited *in vitro* antiproliferative activity against a panel of TNBC cell lines, but not estrogen receptor (ER) or $HER2^+$ cell lines, and this antitumor activity was correlated with a number of cellular parameters that could provide clinically useful tools for identification of sensitive tumors. Furthermore, CB-839 promoted a tumor-specific pharmacodynamic response and had *in vivo* efficacy in breast cancer xenograft models, both as a single agent and in combination with the standard-of-care agent paclitaxel. Together, these results support the notion that glutamine utilization is a critical growth and survival pathway in TNBC and that glutaminase inhibition with CB-839 may provide a therapeutic benefit for patients with TNBC and other glutamine-dependent tumors.

Materials and Methods

Chemistry

BPTES was prepared as previously described (25). The synthesis and chemical characterization of CB-839 (Fig. 1A) is described in ref. (26), wherein it is referenced as #670.

Biochemical analysis

The inhibitory activities of BPTES and CB-839 on recombinant human GAC (rHu-GAC) were measured in a coupled biochemical assay monitoring glutamate production with the NADPH-dependent enzyme glutamate dehydrogenase by a method modified from that described previously (15), as detailed in the Supplementary Methods. To measure time dependence of inhibition, rHu-GAC was preincubated with inhibitor before measurement of glutaminase activity with the coupled assay. Recovery from inhibition after a 90-minute preincubation of rHu-GAC and inhibitor was determined by measuring glutaminase activity at various timepoints following separation of free inhibitor by gel filtration on Zeba Spin Desalting Columns (Thermo Scientific). Glutaminase activity was measured in homogenates prepared from tumor cell lines

and mouse tissues using the coupled assay as described in the Supplementary Methods.

Cellular assays

The breast cell lines, BT-20, BT-549, Hs578T, HCC38, HCC1806, MCF-10A, HCC70, MDA-MB-231, MDA-MB-436, HMC-1–8, HCC1395, HCC1187, Hs739.T, MDA-MB-468, HCC1954, MCF-7, Hs343.T, HCC1428, DU4475, AU-565, T47D, Sk-Br-3, and MDA-MB-175-VII were obtained from the American Type Culture Collection (ATCC). The JIMT-1 and MX-1 cell lines were obtained from the German Collection of Microorganisms and Cell Cultures (DSMZ) and Cell Line Services (CLS), Germany, respectively. All cell lines were passaged for less than 6 months after resuscitation. The ATCC, CLS, and DSMZ cell lines were authenticated by short tandem repeat (STR) analysis. Cell lines for viability, metabolite, glutaminase activity, and Western blot assays were maintained and assayed in RPMI-1640 supplemented with 2 mmol/L glutamine and 10% FBS at 37°C with 5% CO_2 with the exception of the MCF10A which were maintained as described previously (27). For the media depletion and Seahorse assays, HCC1806 and T47D were obtained from the MD Anderson Characterized Cell Line Core [verified using AmpF/STR Identifier kit (Applied Biosystems)] and cultured in Dulbecco's modified Eagle media (DMEM) with 5% FBS at 37°C in 5% CO_2 atmosphere.

For viability assays, all cell lines were treated with CB-839 at the indicated concentrations for 72 hours in duplicate wells and analyzed for antiproliferative effects using Cell Titer Glo (CTG; Promega). For all cell lines except MDA-MB-175, SUM149PT, Hs343.T, HCC38, and BT20 the results presented represent an average across at least two independent experiments. IC_{50} values were calculated using a four parameter curve fit (Graphpad Prism). Relative cell loss or proliferation in the presence of 1 μmol/L CB-839 or in glutamine-free media was determined by comparing the CTG signals measured at time (t) = 72 hours under experimental conditions (CTG_{exp_72}) with both the CTG signal at t = 72 hours for vehicle (0.5% DMSO) treated cells (CTG_{DMSO_72}) and the CTG signal measured at $t = 0$, the time of CB-839 addition or glutamine withdrawal (CTG_0), using the following equations:% cell loss (when $CTG_{exp\_72} < CTG_0$) = $100 \times (CTG_{exp\_72} - CTG_0)/CTG_0$;% cell proliferation (when $CTG_{exp\_72} > CTG_0$) = $100 \times (CTG_{exp\_72} - CTG_0)/(CTG_{DMSO\_72} - CTG_0)$.

Western blot analysis

Lysates were prepared from cell pellets and protein amounts quantitated as described in Supplementary Methods. Lysate proteins (20 μg/lane) were denatured by boiling in SDS-sample buffer, resolved on 7% Tris-acetate gels (together with Novex sharp prestained molecular weight standards; Life Technologies), and transferred to nitrocellulose membranes. Nitrocellulose-immobilized proteins were probed with antibodies recognizing both GAC and KGA forms of glutaminase (1:5,000; AB156876, Abcam), glutamine synthetase (1:1,000; HOOOO2752-M02, Abnova), glutaminase-2 (1:1,000; NBPI-76544, Novus Biologicals), and β-actin (1:10,000; A5441, Sigma-Aldrich) followed by horseradish peroxidse-coupled anti-rabbit or anti-mouse antibodies (1:5,000; NA934V and NA931V, GE Healthcare). Bands were revealed by chemiluminescence (Thermo Scientific) and images were captured with the FluorChem HD2 system (Protein Simple). Further validation of the glutaminase antibody used for Western blotting and the mobility of the bands detected is provided in the Supplementary Methods.

Metabolite and CB-839 measurements by LC/MS

Cell lines or mouse tissues were homogenized in methanol:water (80:20) containing 10 μmol/L $^{13}C_5$, ^{15}N-glutamate as the internal standard and analyzed for metabolite levels by liquid chromatography-tandem mass spectrometry (LC/MS-MS) using the SCIEX API4000 (Applied Biosystems). Mouse tissue homogenates were also analyzed for CB-839 levels using a similar method except that 50 nmol/L carbamazepine was used as the internal standard.

Depletion of substrates in medium

For experiments quantifying metabolite consumption or production in tissue culture media, cells were incubated in DMEM with 5 mmol/L glucose and 0.5 mmol/L glutamine (no serum) for 6 hours. Media concentrations of glucose, lactate, glutamine, and glutamate were quantified using the YSI 2900 Biochemistry Analyzer (YSI Life Sciences).

Seahorse oxygen consumption rates

To quantify rates of oxygen consumption, cells were seeded (8,000 to 10,000 cells/well) in DMEM, 5% FBS, on XF96 V3 PET plates (Seahorse Biosciences). After the cells were attached overnight, the medium was exchanged with DMEM (5 mmol/L glucose with or without 0.5 mmol/L glutamine, no FBS, no bicarbonate). The plates were immediately loaded on the Seahorse XF96 Bioanalyzer (Seahorse Biosciences) for quantification of oxygen consumption rates (OCR). To determine their effects on OCR, compounds were added sequentially (CB-839 or DMSO, 1 μg/mL oligomycin, and 1 μmol/L antimycin).

In vivo studies

CB-839 and metabolite levels were measured in tumors and tissues excised from female Scid/Bg mice (Charles River Laboratories; age 6–9 weeks, 17–23 g) implanted with HCC1806 cells in the mammary fat pad (2.5×10^6 cells/mouse; tumor volume ~500 mm^3 at time of dosing) 4 hours after oral administration of 200 mg/kg CB-839 or vehicle. The vehicle consisted of 25% (w/v) hydroxypropyl-β-cyclodextrin (HPBCD; Roquette) in 10 mmol/L citrate, pH 2. CB-839 was formulated as a solution at 20 mg/mL (w/v) in vehicle; the dose volume for all groups was 10 mL/kg.

Tumor growth studies were done in two xenograft models: (i) a patient-derived TNBC model, where tumor fragments isolated from the breast tissue of a 53-year-old Caucasian woman with stage IIa infiltrating ductal carcinoma (Champions Oncology Model CTG-0052) were implanted subcutaneously into female nu/nu mice (age 4–6 weeks, 19–26 g; Harlan Laboratories) and (ii) a cell line model, where JIMT-1 cells were implanted subcutaneously at 1×10^7 cells per mouse in the flank of female CB.17 SCID mice (age 8–12 weeks, 17–23 g; Charles River Laboratories). In both models, when tumors reached approximately 100–150 mm^3, mice were dosed with vehicle (as described above) or 200 mg/kg CB-839 ($n = 10$/group) prepared in vehicle orally twice daily every 12 hours for 28 to 35 days. For the JIMT-1 model, two additional cohorts were dosed with paclitaxel prepared in 5% ethanol/5% Cremophor EL given as an intravenous bolus at 10 mg/kg every other day for 5 doses alone or in combination with 200 mg/kg CB-839 dosed orally twice daily. Tumor volumes and body weights were measured twice weekly.

Results and Discussion

CB-839 is a potent and selective glutaminase inhibitor

The small-molecule BPTES was previously described as an allosteric glutaminase inhibitor active against both splice variants of the *GLS* gene, *GAC* and *KGA* (reported Ki between 0.2 and 3 μmol/L), but not the liver form of glutaminase, encoded by the *GLS2* gene (18, 19, 21, 22). CB-839 (Fig. 1A) is a novel glutaminase inhibitor that exhibits low nanomolar potency in biochemical and cellular assays and has good oral bioavailability. In a biochemical assay with recombinant human GAC (rHu-GAC), the potency and kinetic behavior of CB-839 was distinct from BPTES. Unlike BPTES, CB-839 exhibited time-dependent (Fig. 1B and C) and slowly reversible kinetics (Fig. 1D). IC_{50} values for glutaminase inhibition by CB-839 following preincubation with rHu-GAC for ≥1 hour were < 50 nmol/L, at least 13-fold lower than with BPTES. Furthermore, upon removal of free inhibitor, recovery of rHu-GAC activity was rapid for BPTES (<3 minutes) and slow for CB-839 ($t_{1/2} = 45$ minutes at 25°C). This altered kinetic behavior was also associated with a change in the mode of inhibition. BPTES displayed a predominantly uncompetitive mechanism characterized by dose-dependent decreases in both V_{max} and the K_m for glutamine (Supplementary Fig. S1A) and a shift toward greater potency with increasing glutamine concentrations (Supplementary Fig. S1C), consistent with previous reports (18, 21). In contrast, CB-839 behaved as a primarily noncompetitive inhibitor impacting V_{max} but with minimal effect on K_m (Supplementary Fig. S1B) and displaying potency that was independent of glutamine concentration (Supplementary Fig. S1D). The ability of CB-839 to inhibit native glutaminase in mouse tissue homogenates was also measured using a coupled biochemical assay (see Materials and Methods). Treatment of homogenates prepared from kidney and brain, two tissues that express the *GLS* gene products (28, 29), with CB-839 for 1 hour resulted in glutaminase inhibition ($IC_{50} = 20$–30 nmol/L) comparable to that obtained with rHu-GAC (Fig. 1E). In contrast, similar treatment of a mouse liver homogenate which contains primarily the *GLS2* gene product (28, 29) with CB-839 resulted in no detectable glutaminase inhibition. This result is consistent with the reported high degree of selectivity of BPTES for *GLS* over *GLS2* gene products (18, 22). Taken together, these results demonstrate that although CB-839 and BPTES shares a similar allosteric binding mechanism and selectivity profile, CB-839 has increased potency and distinct kinetic behavior, exhibiting a slow-on/slow-off mechanism.

CB-839 blocks glutamine utilization in TNBC cells

TNBC primary tumors and many cell lines are reported to have high expression of glutaminase (*GLS* gene products) and low expression of glutamine synthetase (*GLUL* gene product), an enzyme that produces glutamine from glutamate (14, 16). This expression pattern is associated with high glutamine consumption and a dependence of TNBC cell line growth on exogenous glutamine, suggesting that TNBC would be sensitive to glutaminase inhibition. To test this hypothesis, the metabolic consequences of glutaminase inhibition with CB-839 were examined in two TNBC cell lines, HCC1806 and MDA-MB-231, and one $ER^+/HER2^-$ line, T47D. CB-839 treatment had a potent effect on the proliferation of the two TNBC cell lines (IC_{50} of 20–55 nmol/L associated with cell loss at >100 nmol/L) but no effect on the viability of T47D cells (Fig. 2A and Supplementary Fig. S2A and S2B). BPTES also exhibited selective antiproliferative activity on the two TNBC cell lines (Supplementary Fig. S2B) but with an IC_{50} of ≥2 μmol/L, consistent with its weaker potency in biochemical assays. To confirm that treatment with 1 μmol/L CB-839 was inhibiting the metabolism of glutamine, the rates of glutamine consumption and glutamate production were quantified for HCC1806 and T47D cell lines (Fig. 2B). As expected for a glutaminase inhibitor, the rates of glutamine consumption were reduced for both lines. Importantly, the relatively high baseline glutamine consumption rate exhibited by HCC1806 cells was completely inhibited by CB-839 demonstrating the absolute requirement of glutaminase activity to metabolize glutamine in this cell line. In contrast, glutamine consumption was only partially inhibited in T47D cells suggesting that these cells are capable of metabolizing glutamine through glutaminase-independent pathways.

Like the glutamine consumption rates, glutamate production rates were also dramatically reduced for HCC1806 cells after CB-839 treatment. The glutaminase-dependent link between glutamine consumption and glutamate production in this cell line is further highlighted by their nearly identical CB-839 IC_{50} values (Fig. 2C). This association was not observed for T47D cells; the untreated glutamate production rate was lower than that of HCC1806 cells but not significantly altered by CB-839

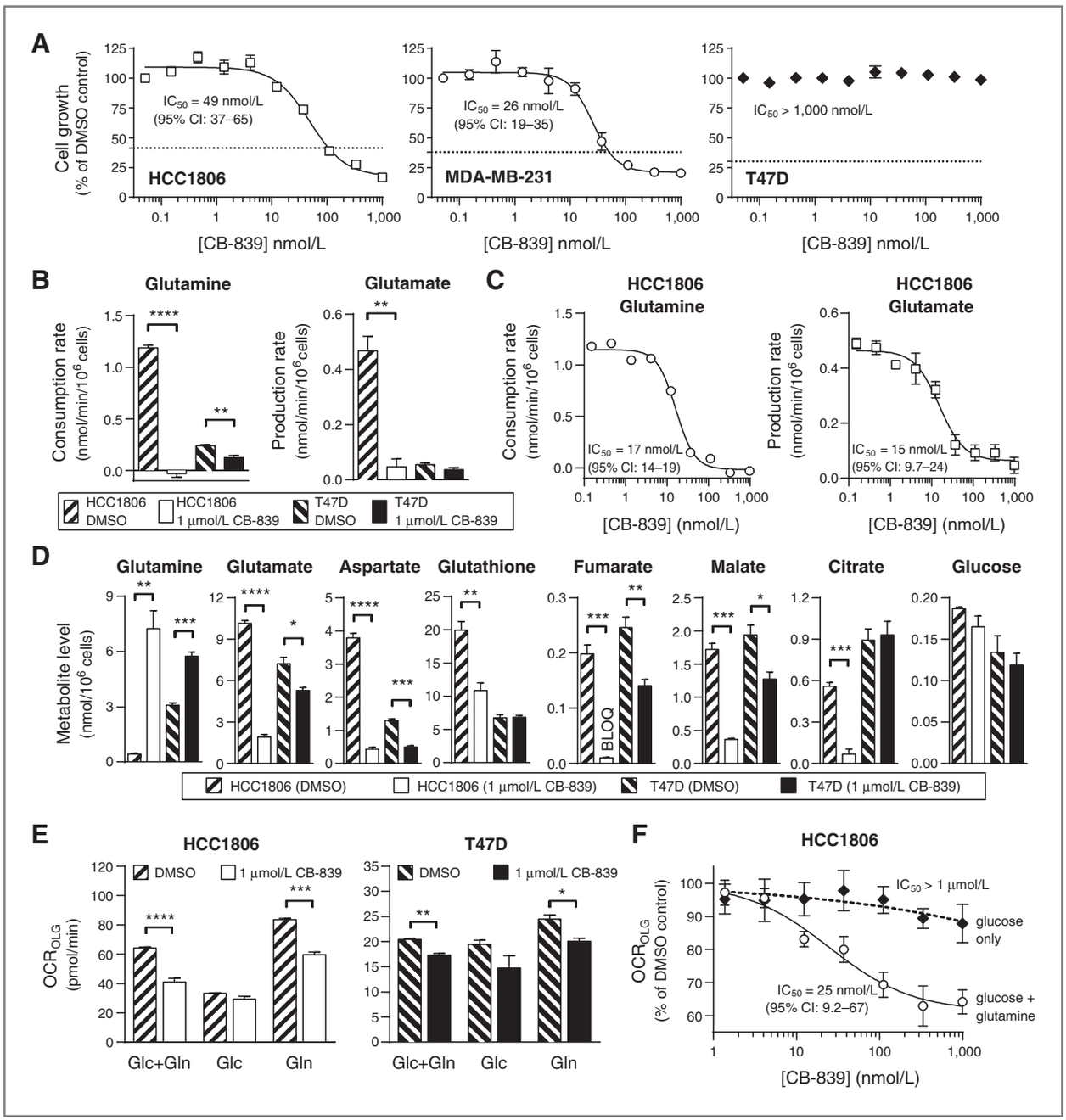

Figure 2. Glutaminase inhibition with CB-839 has antiproliferative activity in TNBC cells that is associated with decreased glutamine utilization. A, cell proliferation dose–response curves for HCC1806, MDA-MB-231, and T47D cells treated with CB-839 for 72 hours. The dashed line indicates the relative Cell Titer Glo signal at the time of CB-839 addition. B, glutamine consumption and glutamate production rates for HCC1806 and T47D measured after DMSO or 1 μmol/L CB-839 treatment. Medium was collected after 6 hours of treatment and analyzed for glutamine and glutamate with the YSI 2900 Biochemistry Analyzer. C, dose–response curves for glutamine consumption and glutamate production rates by HCC1806 cells treated with CB-839 for 6 hours. D, intracellular metabolite levels measured in HCC1806 and T47D cells treated with DMSO or 1 μmol/L CB-839 for 4 hours. The level of fumarate in the CB-839 treated HCC1806 cells was below the limit of quantitation (BLOQ) of ~0.01 nmol per 10^6 cells. E, oligomycin-dependent oxygen consumption rate (OCR_{OLG}) for HCC1806 and T47D cells measured after 80 minutes of DMSO or 1 μmol/L CB-839 treatment in media containing 5 mmol/L glucose (Glc) with and without 0.5 mmol/L glutamine (Gln). OCR_{OLG} was used to determine the contribution of ATP-synthase to OCR. F, dose–response of OCR_{OLG} after 80 minutes of CB-839 treatment for HCC1806 in glucose plus glutamine or glucose-only containing media. For all panels, the mean and SEM of at least duplicate measurements are plotted. Results are representative of at least two independent experiments. Nonlinear 4 parameter dose–response curve fits were used to calculate IC_{50} and 95% CI. Comparisons of treated and untreated conditions were performed by unpaired *t* test: *, $P \leq 0.05$; **, $P \leq 0.01$; ***, $P \leq 0.001$; ****, $P \leq 0.0001$.

(Fig. 2B). These results suggest that glutamine metabolized by glutaminase was the major source of glutamate production in HCC1806 but not in T47D cells. Neither glucose consumption nor lactate production rates were substantially impacted in either cell line, supporting the glutamine specificity of CB-839 effects and the lack of potential compensatory changes in glycolysis when glutaminase is inhibited (Supplementary Fig. S2C).

The effect of glutaminase inhibition on the levels of intracellular metabolites was also examined in these cell lines. In addition to the expected effects on glutamine (accumulation of substrate) and glutamate (depletion of product), CB-839 reduced the concentration of a number of key metabolites downstream of glutamate within 4 hours (Fig. 2D) and maintained these effects for 24 hours (Supplementary Fig. 2D). In contrast, no changes were observed in cellular glucose levels. Among the downstream metabolites impacted by CB-839 were: (i) aspartate (linked to glutamate through aspartate aminotransferase); (ii) glutathione (for which glutamate is a key precursor); and (iii) the TCA cycle intermediates fumarate, malate, and citrate (via the anapleurotic role of glutamate in producing the TCA cycle intermediate α-ketoglutarate). Importantly, in all cases the magnitude of the CB-839 effect on downstream metabolites was greater in the TNBC cell line (HCC1806) than in the ER^+ cell line (T47D), consistent with a greater dependence on glutaminase in TNBC. Similar results were obtained with the other TNBC cell line, MDA-MB-231 (Supplementary Fig. S2E and data not shown), where the EC_{50} of glutamine accumulation and IC_{50} of glutamate depletion were tightly correlated, as noted previously for glutamine consumption and glutamate production in HCC1806. Across a panel of breast cancer cell lines, the ability of CB-839 to raise glutamine levels and lower glutamate levels was generally greater for TNBC cells than receptor-positive cells (Supplementary Fig. S2F and S2G). These effects on intracellular metabolite pools are consistent with those previously described for glutaminase siRNA knockdown and BPTES (7, 8, 11). Highlighting the functional importance of metabolic intermediates derived from glutamate, cell permeable forms of TCA cycle intermediates (oxaloacetate and α-ketoglutarate) and glutathione partially or fully reversed the suppression of TNBC cell viability mediated by CB-839 (Supplementary Fig. S2H). However, due to the potential metabolic interconversion of these reagents, additional studies will be required to determine which pathways are most critical for maintenance of cell viability.

Reduction in intracellular concentrations of TCA cycle intermediates suggested that mitochondrial function might be impaired by CB-839 treatment. To test this hypothesis, the oxygen consumption rates with CB-839 treatment were quantified for HCC1806 and T47D cell lines using a Seahorse Bioanalyzer with different combinations of nutrients in the medium (glucose and/or glutamine). For media containing glutamine, ATP synthase–dependent oxygen consumption (OCR_{OLG}) was reduced after 80-minute treatment with CB-839 (Fig. 2E). As with the measures of growth inhibition and other metabolic responses, the most pronounced OCR_{OLG} responses were with HCC1806 cells. This impaired mitochondrial function was associated with reduction of glutamine consumption as shown by the similar IC_{50} values (Fig. 2C and F). Importantly, the actions of CB-839 were consistent with selective glutaminase inhibition; reduction in OCR_{OLG} was dependent on the presence of glutamine as a substrate in the medium (Figs. 2E and F).

Overall, the impact of CB-839 on cellular metabolism supports an on-target mechanism of action and high degree of TNBC selectivity. The differential effects of CB-839 on glutathione levels were particularly striking. This may reflect the fact that glutamate contributes to glutathione production both as a direct precursor and as a cofactor in the import of cysteine, another glutathione precursor, via the system x_c- glutamate/cystine antiporter (30). Importantly, glutathione concentrations were reduced in HCC1806 but not T47D, demonstrating that certain metabolites derived from glutamine may be independent of glutaminase function in ER^+ cancers. Interestingly, a large fraction of glutamate generated from glutamine by glutaminase in HCC1806 cells was recovered in the media, perhaps due to a high demand for cysteine in these TNBC cells (14). Additional metabolite flux studies will help to elucidate more precisely the impact of CB-839 on metabolic pathways downstream of glutamine.

GAC expression and glutaminase activity are elevated in TNBC

To expand upon the reported differential expression of glutamine metabolic genes across breast cancer subtypes (14, 16), we investigated the expression of glutaminase isoforms (*GAC* and *KGA* splice forms of *GLS* plus *GLS2*) and *GLUL* in the breast invasive carcinoma dataset from The Cancer Genome Atlas (TCGA) and the breast cancer cell lines in The Cancer Cell Line Encyclopedia (CCLE; refs. 31, 32). Expression levels were compared across TNBC and receptor-positive subtypes (comprised of $ER^+/HER2^+$, $ER^+/HER2^-$ and ER^-/HER^+) as well as, in the case of the TCGA dataset, normal breast tissue (Supplementary Fig. S3A and S3B). These large datasets yielded expression patterns consistent with previous reports (14, 16), including elevated *GLUL* in primary ER^+ tumors. Importantly, the elevated *GLS* expression in TNBC reported by Kung and colleagues (16) appears to be largely due to the *GAC* splice variant, consistent with a recent report (14). Average *GAC* expression was elevated in TNBC primary tumors relative to both normal breast tissue and receptor-positive tumor subtypes. In contrast, there was no difference in *KGA* expression between TNBC and normal tissue. *GAC* and *KGA* expression were both lower in receptor-positive tumors either in comparison to TNBC tumors or normal tissue. These data indicate a selective upregulation of *GAC* in TNBC with a coordinated downregulation of both *GLS* splice variants in receptor-positive tumors. As in the primary tumor dataset, TNBC

cell lines in the CCLE dataset had higher *GAC* and lower GLUL expression than the receptor-positive cell lines. Although *GLS2* expression was lower in primary TNBC tumors relative to both normal breast tissue and receptor-positive tumors, expression of *GLS2* in cell lines was low and independent of receptor status.

To determine whether these gene expression patterns were reflected at the protein level, a panel of breast cell lines was analyzed by Western blot analysis for the expression of GAC, KGA, GLUL, and GLS2 (Fig. 3A). Consistent with the mRNA expression, the majority of TNBC cell lines expressed high levels of both GAC and KGA in comparison with receptor-positive lines. Interestingly, the exceptions were JIMT-1 and HCC1954, both basal-like $ER^-/HER2^+$ cell lines (27, 33), consistent with recent observations that molecular subtypes can also distinguish glutaminase expression patterns (14). The expression of GLUL and GLS2 was more variable and did not display a clear distinction between TNBC and receptor-positive cell lines. Consistent with the GAC and KGA mRNA and protein expression levels, phosphate-activated glutaminase specific activities in lysates prepared from the same breast cancer cell line panel were elevated in TNBC cell lines as compared with the receptor-positive cells (Fig. 3B and Supplementary Fig. S4A).

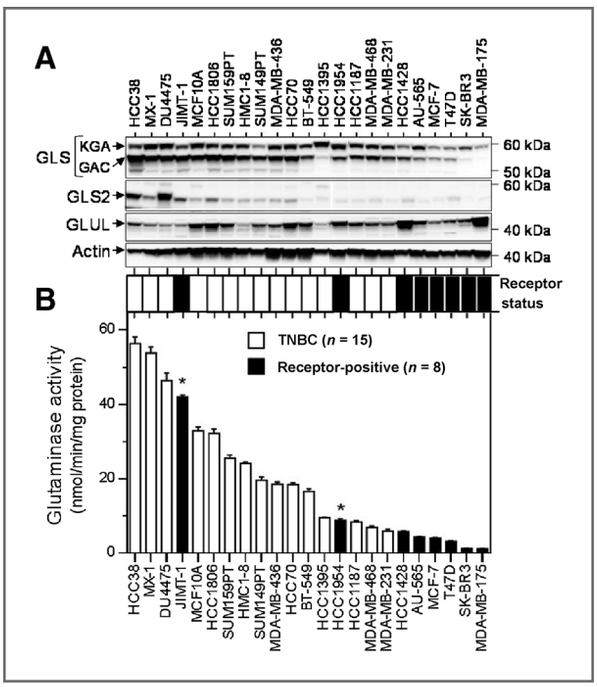

Figure 3. TNBC cell lines have elevated glutaminase protein and activity levels. A, SDS-PAGE and immunoblot analyses of a breast cancer cell line panel using antibodies that recognize GAC, KGA, GLS2, and GLUL. GAC and KGA, recognized by the same antibody, are distinguishable by their molecular weight difference as indicated with arrows. Blots were reprobed with an antibody recognizing β-actin as a loading and transfer control (shown only for the GAC/KGA blot). B, phosphate-activated glutaminase activity was measured in cell line homogenates and normalized to protein amount used in the assay; mean and SEM from duplicate measurements are plotted. Results are representative of two independent experiments. The basal-like $ER^-/HER2^+$ cell lines JIMT-1 and HCC1954 are annotated with asterisks (*).

TNBC cell lines are sensitive to glutaminase inhibition with CB-839

The elevated levels of glutaminase detected in TNBC indicate that this subset of breast tumors may exhibit enhanced sensitivity to glutaminase inhibition with CB-839. To test this hypothesis, the antiproliferative effects of CB-839 across a panel of 28 breast cancer cell lines (20 TNBC, 4 $ER^+/HER2^-$, and 4 $ER^-/HER2^+$) was evaluated. Potent antiproliferative IC_{50} values for CB-839 (2–300 nmol/L) were observed with most of the TNBC cell lines while all but two of the receptor-positive lines had an $IC_{50} > 1$ μmol/L (Fig. 4A). Similarly, the TNBC cell lines exhibited greater sensitivity as measured by the extent of cell growth or cell loss (i.e., a decrease in cell number relative to the time of compound addition) following treatment with 1 μmol/L CB-839 for 72 hours (Fig. 4B and Supplementary Fig. S4B). Cell loss was observed in the majority of TNBC cell lines; the remaining TNBC cell lines and the basal-like $HER2^+$ cell lines showed a decrease in cell proliferation relative to the DMSO control. No cell loss was observed in the other receptor-positive cell lines, although a 40% to 55% decrease in proliferation was observed in two of them. In TNBC cell lines, cell loss was associated with induction of apoptosis, as evidenced by caspase-3/7 activation (Supplementary Fig. S5), consistent with apoptosis induction following glutamine withdrawal in a subset of breast cell lines (14).

To determine whether the sensitivity of breast cancer cell lines to CB-839 is correlated with their dependence on glutamine, the effect of glutamine withdrawal was tested across the breast cancer cell line panel. The TNBC cell lines exhibited greater overall dependence on glutamine (Fig. 4C and Supplementary Fig. S4C), as noted previously (14, 16), with the majority of TNBC cell lines showing cell loss when deprived of glutamine (Fig. 4C). Importantly, across this cell line panel, sensitivity to glutaminase inhibition with CB-839 was highly correlated with dependence on glutamine (Fig. 4D), suggesting that glutamine supports TNBC cell viability primarily through its glutaminase-mediated conversion to glutamate.

GAC expression, glutaminase activity, and metabolite levels predict sensitivity to CB-839

We hypothesized that the genetic signature that distinguishes TNBC from receptor-positive tumors and normal tissue could be used to identify tumors sensitive to CB-839 treatment. Indeed, across the breast cancer cell line panel, greater sensitivity to CB-839 with regard to proliferation or viability was correlated with higher *GAC* expression (Fig. 5A). Although CB-839 inhibits both splice variants of *GLS*, no correlation between CB-839 sensitivity and *KGA* expression was observed, supporting a dominant role for the *GAC* splice variant in the glutamine utilization and dependence of TNBC cell lines. Although the functional distinctions between the *GLS* splice variants remains to be

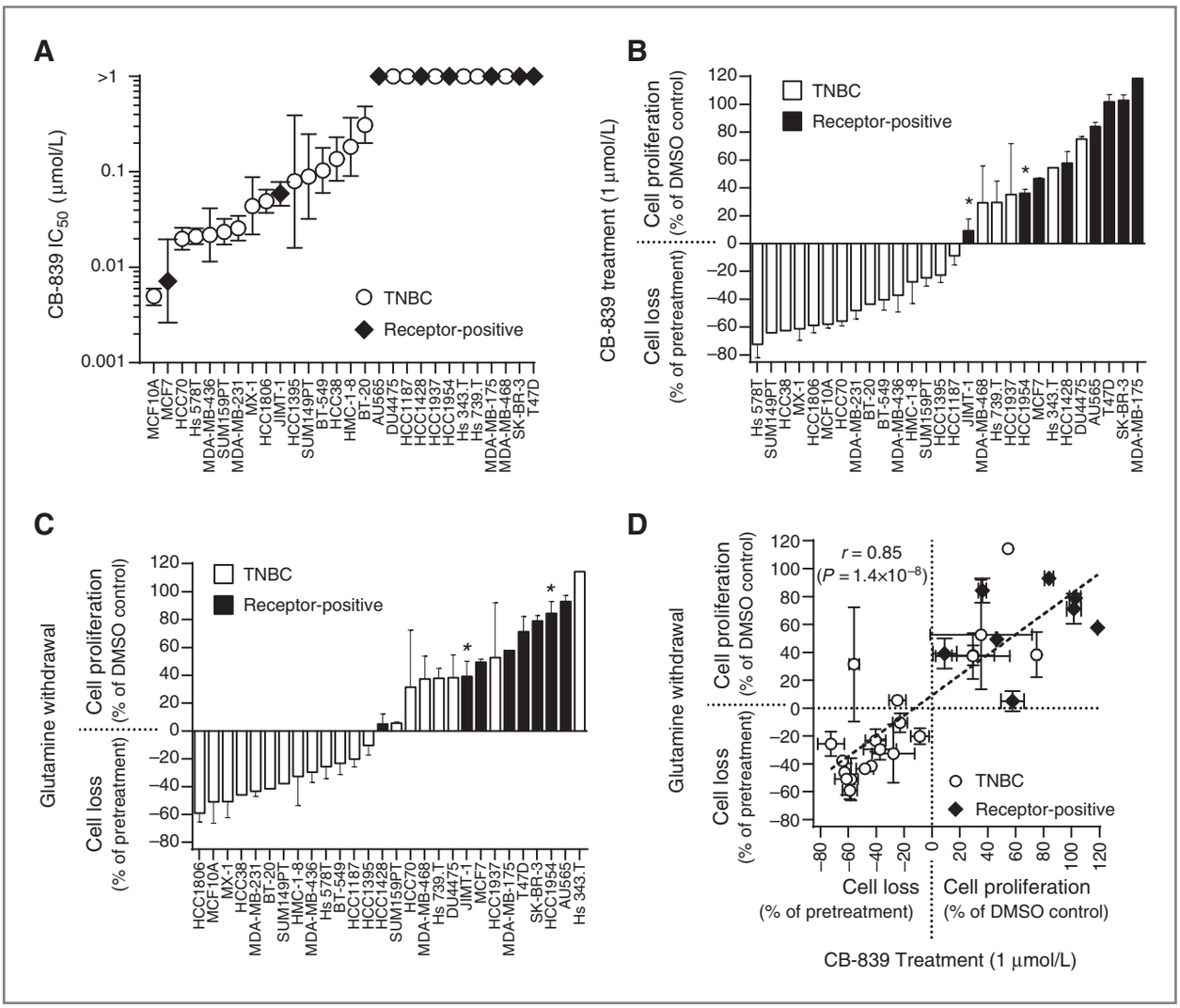

Figure 4. The antiproliferative activity of CB-839 on breast cancer cell lines is correlated with their dependence on glutamine for growth and survival. A, antiproliferative IC_{50} values measured on a panel of breast cancer cell lines treated with CB-839 for 72 hours. The mean and 95% CI of at least duplicate measurements are shown. B, cell proliferation or loss measured in breast cell lines after treatment with 1 μmol/L CB-839 for 72 hours. The mean and SEM of at least duplicate measurements are shown. C, cell proliferation or loss measured in breast cell lines after 72 hours in glutamine-free media. The mean and SEM of at least duplicate measurements is plotted. D, correlation between cell proliferation or loss measured after CB-839 treatment from A plotted on the *x*-axis and glutamine withdrawal from B plotted on the *y*-axis. Each datapoint depicts an individual cell line. The Pearson correlation coefficient (*r*) and corresponding *P* value is shown. The dashed line is the linear regression fit. The zero value (B–D) represents the cell density at the time of compound addition. For all panels, $n = 20$ TNBC cell lines and $n = 8$ receptor-positive cell lines. For B and C, the basal-like $ER^-/HER2^+$ cell lines JIMT-1 and HCC1954 are annotated with asterisks (*).

established, it is possible that potential differences in activity, regulation, or localization make GAC more efficient at supporting a transformed phenotype (6, 15, 22, 23). In support of this possibility, siRNA knockdown studies in NSCLC have shown that the *GAC* splice variant of *GLS*, but not *KGA*, has an important role supporting tumor cell growth (10).

To expand upon this genetic correlation, the relationship between CB-839 sensitivity and measures of glutaminase function were evaluated across the breast cancer cell line panel. The functional markers evaluated included glutaminase-specific activity (see Fig. 3B), the baseline ratio of intracellular glutamate to glutamine (product to substrate ratio serving as a potential surrogate for glutaminase activity), and the extent to which 1 μmol/L CB-839 promoted accumulation of cellular glutamine or depletion of cellular glutamate (as noted in Fig. 2D). Greater CB-839 sensitivity was strongly correlated with higher glutaminase specific activity, the most direct functional readout (Fig. 5B). Consistent with greater glutamine utilization by TNBC cells, each of the metabolite-based functional markers was significantly elevated in the TNBC cell lines relative to the receptor-positive cell lines (Supplementary Figs. S4D–S4F and

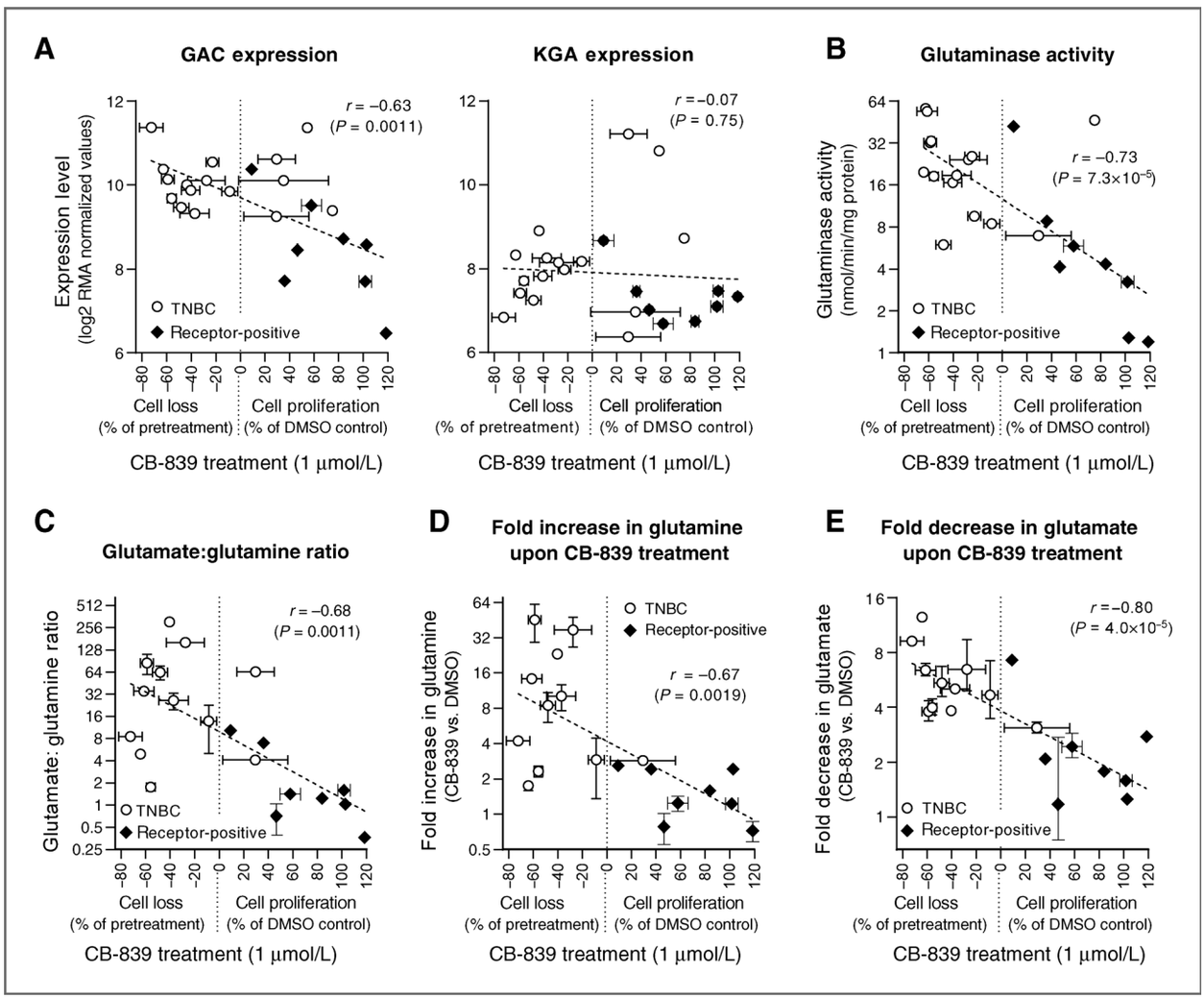

Figure 5. Correlation of CB-839 sensitivity with *GAC* expression, glutaminase activity, and metabolite levels. A, correlation between cell proliferation or loss measured after CB-839 treatment (from Fig. 4B) plotted on the *x*-axis and *GAC* (left) or *KGA* (right) mRNA expression from the CCLE database (log2 RMA normalized values) plotted on the *y*-axis. B, correlation between cell proliferation or loss measured after CB-839 treatment as in A plotted on the *x*-axis and glutaminase specific activity from Fig. 3B plotted on the *y*-axis. C, correlation between cell proliferation or loss measured after CB-839 treatment as in A plotted on the *x*-axis and the baseline ratio of intracellular glutamate to glutamine plotted on the *y*-axis. D, correlation between cell proliferation or loss measured after CB-839 treatment as in A plotted on the x-axis and the fold increase in intracellular glutamine upon treatment with 1 μmol/L CB-839 for 4 hours plotted on the *y*-axis. E, correlation between cell proliferation or loss measured after CB-839 treatment as in A plotted on the *x*-axis and the fold decrease in intracellular glutamate upon treatment with 1 μmol/L CB-839 for 4 hours plotted on the *y*-axis. For all panels, each datapoint depicts the mean and SEM from at least duplicate measurements for an individual cell line. The zero value on the *x*-axis represents the cell density at the time of compound addition and the dashed line is the linear regression fit (using log2-transformed values in B–E). The calculated Pearson correlation coefficients (*r*) and associated *P* values are shown. For receptor-positive cell lines, $n = 8$ for all panels; for TNBC cell lines, $n = 16$ for A, $n = 15$ for B, and $n = 12$ for C–E.

S6A–S6C). Accordingly, greater CB-839 sensitivity was associated with higher baseline cellular glutamate to glutamine ratio (Fig. 5C), greater CB-839–induced cellular glutamine accumulation (Fig. 5D), and greater CB-839–induced cellular glutamate depletion (Fig. 5E). Taken together, these observations demonstrate that across a breast cancer cell line panel, sensitivity to CB-839 is correlated with both genetic (*GAC* expression) and functional markers (glutaminase activity, glutamate: glutamine ratio) of glutamine utilization. Importantly, evaluation of these biomarkers of CB-839 sensitivity in tumor biopsies in the clinic could be used to select patients with the greatest likelihood to respond to CB-839 treatment.

Oral dosing of CB-839 inhibits tumor glutaminase activity and changes metabolite levels

The *in vivo* utility of CB-839 was initially evaluated in pharmacodynamic studies. CB-839 was administered orally at a dose of 200 mg/kg to scid/beige mice bearing orthotopically implanted HCC1806 tumors. Tumor, plasma, and selected tissues were collected 4 hours after

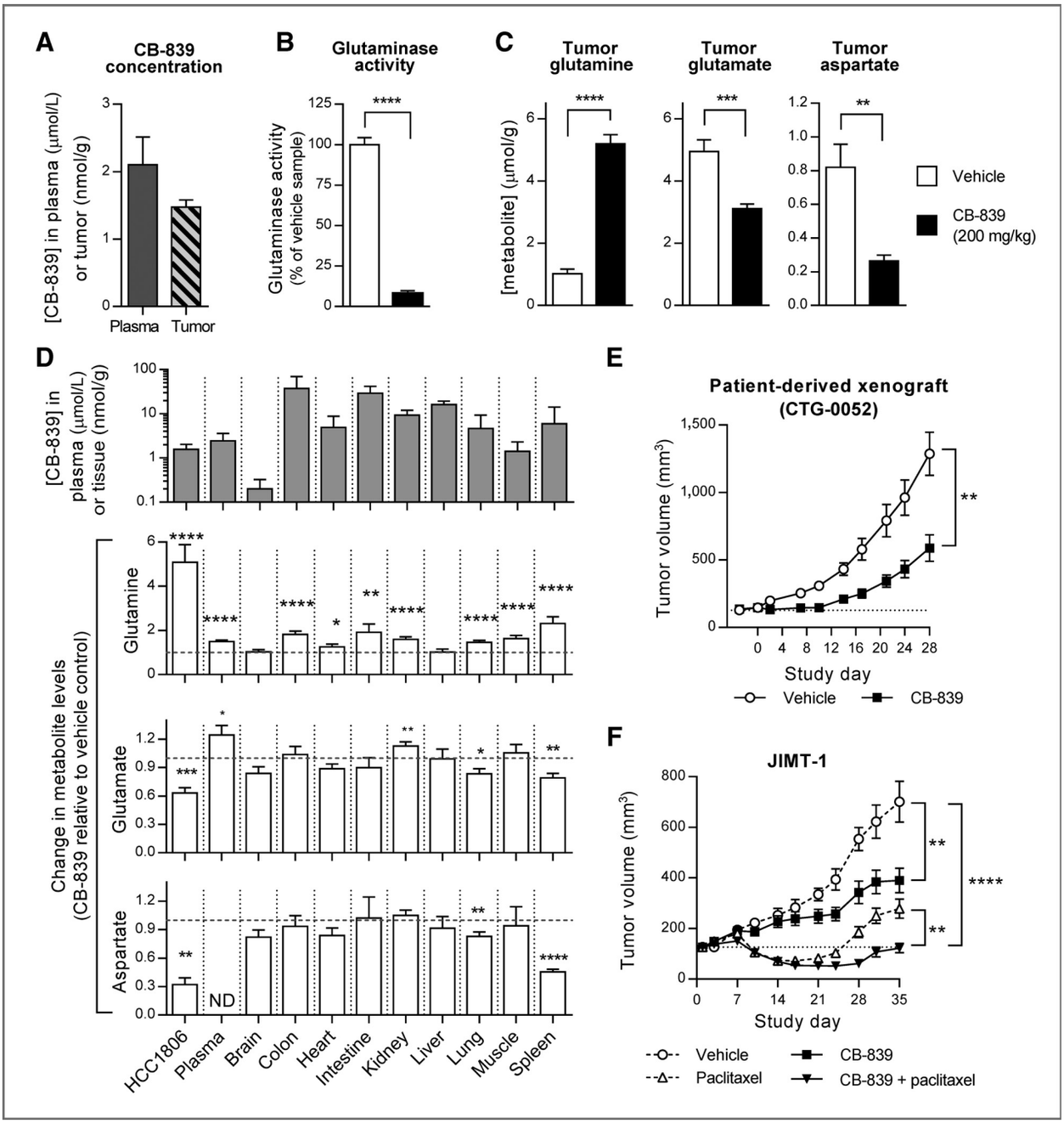

Figure 6. Oral dosing of CB-839 inhibits glutaminase in TNBC xenograft tumors and has antitumor activity in patient-derived TNBC and JIMT-1 cell line xenograft models. A, CB-839 levels measured by LC/MS-MS in plasma and tumor samples 4 hours after oral dosing of 200 mg/kg CB-839 to mice bearing HCC1806 tumors ($n = 10$ per group). B, glutaminase activity measured in tumor lysates from animals ($n = 5$ per group) treated with vehicle or CB-839 as in A. The percent inhibition by CB-839 relative to vehicle is plotted. C, metabolite levels measured by LC/MS-MS in tumor lysates from animals ($n = 10$ per group) treated with vehicle or CB-839 as in A. D, CB-839 (top graph) and metabolite levels (bottom graphs) measured by LC/MS-MS in plasma, normal tissue, or tumor extracts from animals ($n = 10$ per group) treated with vehicle or CB-839 as in A. For metabolites, the fold increase or decrease after CB-839 treatment relative to the vehicle control is plotted; dotted line at $y = 1$ denotes no change in metabolite levels. E, tumor volumes measured in a TNBC patient-derived xenograft model ($n = 10$ per group) dosed orally with vehicle or 200 mg/kg CB-839 twice daily (BID) for 28 days. F, tumor volumes measured in a JIMT-1 cell line xenograft model as in E but with two additional cohorts: paclitaxel at 10 mg/kg given as an intravenous bolus every other day for 5 doses administered alone or in combination with CB-839. For all panels, mean and SEM values are plotted. Statistical analyses of CB-839–treated in comparison with control groups were performed by unpaired t test: *, $P \leq 0.05$; **, $P \leq 0.01$; ***, $P \leq 0.001$; ****, $P \leq 0.0001$.

dosing for measurement of CB-839 levels, pharmacodynamic markers (glutamine, glutamate, and aspartate), and glutaminase activity (tumor only). Plasma and tumor CB-839 concentrations of > 1.5 μmol/L or nmol/g, respectively, were achieved demonstrating good systemic exposure (Fig. 6A). This level of exposure was associated with a robust pharmacodynamic response in the tumor as measured by the suppression of glutaminase activity (Fig. 6B) and the increase in glutamine and decreases in glutamate and aspartate (Fig. 6C) in tumor lysates. Furthermore, CB-839 achieved widespread exposure in most mouse tissues (Fig. 6D). The exception was brain where exposure was >7-fold lower than tumor or other tissues, indicating that CB-839 does not efficiently cross the blood–brain barrier. Systemic CB-839 exposure was associated with an increase in glutamine in plasma and all tissues with the exception of brain, where exposure was likely limiting, and liver, where the CB-839 insensitive form of glutaminase, *GLS2*, is expressed (Fig. 6D). However, despite high CB-839 exposure, the glutamine increases in plasma and tissues (maximum 2.3-fold in spleen) were not as dramatic as those in tumor (>5-fold). Similarly, in most tissues, CB-839 failed to reduce glutamate or aspartate levels; in the two tissues where glutamate and aspartate reductions were observed (lung and spleen), they were less pronounced than those seen in tumors. Together, these results suggest that the pharmacodynamic impact of CB-839 is largely tumor-selective, perhaps due to greater flux through the glutaminase pathway in tumors or efficient compensatory mechanisms in normal tissues.

CB-839 has antitumor activity in xenograft models of TNBC and basal-like breast cancer

The antitumor activity of CB-839 was tested in two breast cancer xenograft models, a primary patient-derived TNBC xenograft and a cell line-based xenograft model using the $HER2^+$ basal-like cell line JIMT-1. The primary patient-derived TNBC model was selected based on high *GAC* expression, high glutaminase activity, and a high ratio of glutamate to glutamine relative to a panel of other breast tumors and other solid tumors (data not shown). CB-839 was administered at 200 mg/kg twice daily once the subcutaneously implanted tumors reached 150 mm^3. Because CB-839 clearance was relatively high in mice (Supplementary Fig. S7A), twice daily administration was necessary to maintain continuous target coverage. In this model, single agent CB-839 suppressed tumor growth by 61% relative to vehicle control at the end of study ($P = 0.0029$; Fig. 6E).

In the JIMT-1 xenograft model, the antitumor efficacy was evaluated by treating established tumors (125 mm^3 at the start of dosing) with CB-839 both as a single agent and in combination with paclitaxel, a standard-of-care chemotherapeutic agent for the treatment of TNBC. The regimen for paclitaxel (five doses at 10 mg/kg delivered every other day at the start of study) was chosen to provide suboptimal efficacy to ensure a window to evaluate the potential impact of combination treatment. Oral dosing of CB-839 alone (200 mg/kg twice daily) resulted in 54% tumor growth inhibition (TGI) relative to vehicle control at study end ($P = 0.004$; Fig. 6F). Single agent paclitaxel caused an initial regression of the JIMT-1 tumors that was followed by a rapid regrowth resulting in a TGI of 73% relative to vehicle control at the end of study ($P = 0.0002$). Combination of CB-839 with paclitaxel largely suppressed the regrowth of the tumors resulting in a TGI relative to vehicle control of 100% at the end of study ($P < 0.0001$ vs. vehicle and $P = 0.0025$ vs. paclitaxel alone). These *in vivo* efficacy results build upon those previously published using other glutaminase inhibitors in lymphoma and renal cancer models (6, 9, 13, 19).

In both xenograft studies, CB-839 was well tolerated (even in combination with paclitaxel), with no difference in weight gain between groups (Supplementary Fig. S7B and S7C) and no overt signs of toxicity. This tolerability profile may be reflective of modest pharmacodynamic effects of CB-839 in normal tissues in comparison with tumor (Fig. 6D), and suggests that this agent may have a favorable therapeutic index in the clinic.

Conclusion

We report here the discovery and characterization of CB-839, a potent and selective inhibitor of glutaminase. CB-839 displays on-target cellular activity as indicated by its ability to suppress key glutamate-derived metabolic intermediates that support macromolecule synthesis, ATP production, and cellular redox balance. Our work demonstrates that TNBC cells are particularly dependent on glutamine for growth and survival and that blocking this pathway by inhibiting the activity of glutaminase with CB-839 has antitumor activity in both *in vitro* and *in vivo* models. This activity is correlated with elevated expression of the *GAC* splice variant of glutaminase and a high baseline ratio of glutamate to glutamine (product to substrate), two markers that could be used to enrich for responsive patients in clinical trials. Together, these results suggest that CB-839 may have therapeutic benefit for patients with TNBC and perhaps other glutamine-dependent cancers by selectively blocking the ability of tumor cells to use glutamine as a nutrient.

Disclosure of Potential Conflicts of Interest

No potential conflicts of interest were disclosed.

Authors' Contributions

Conception and design: M.I. Gross, S.D. Demo, J.B. Dennison, L. Chen, B. Goyal, G.J. Laidig, E.R. Lewis, A.L. MacKinnon, F. Parlati, E.B. Sjogren, T.F. Stanton, M.K. Bennett

Development of methodology: S.D. Demo, J.B. Dennison, T. Chernov-Rogan, J.R. Janes, E.R. Lewis, A.L. MacKinnon, F. Parlati, J. Yang

Acquisition of data (provided animals, acquired and managed patients, provided facilities, etc.): M.I. Gross, S.D. Demo, J.B. Dennison, T. Chernov-Rogan, J.R. Janes, E.R. Lewis, J. Li, A.L. MacKinnon, F. Parlati, M.L.M. Rodriguez, P.J. Shwonek, T. Wang, J. Yang, F.Y. Zhao

Analysis and interpretation of data (e.g., statistical analysis, biostatistics, computational analysis): S.D. Demo, J.B. Dennison, E.R. Lewis, A.L. MacKinnon, F. Parlati, M.L.M. Rodriguez, M.K. Bennett

Writing, review, and/or revision of the manuscript: M.I. Gross, S.D. Demo, J.B. Dennison, T. Chernov-Rogan, A.L. MacKinnon, F. Parlati, M.K. Bennett
Administrative, technical, or material support (i.e., reporting or organizing data, constructing databases): S.D. Demo, J.R. Janes, J. Li, F. Parlati
Study supervision: J.R. Janes, F. Parlati, M.K. Bennett

Acknowledgments

The authors thank Dr. Norman P. Curthoys (Colorado State University) for the kind gift of anti-KGA rabbit polyclonal antibody and helpful discussions and Terri Davis and Barbara Frauman for help with manuscript preparation.

Grant Support

J.B. Dennison is supported by a GlaxoSmithKline TRIUMPH postdoctoral fellowship, the American Cancer Society, and Joe and Jessie Crump Medical Research Fund Postdoctoral Fellowship. All other work was funded by Calithera Biosciences, Inc.

The costs of publication of this article were defrayed in part by the payment of page charges. This article must therefore be hereby marked *advertisement* in accordance with 18 U.S.C. Section 1734 solely to indicate this fact.

Received October 29, 2013; revised February 4, 2014; accepted February 4, 2014; published OnlineFirst February 12, 2014.

References

1. Vander Heiden MG, Cantley LC, Thompson CB. Understanding the Warburg effect: the metabolic requirements of cell proliferation. Science 2009;324:1029–33.
2. Koppenol WH, Bounds PL, Dang CV. Otto Warburg's contributions to current concepts of cancer metabolism. Nat Rev Cancer 2011;11:325–37.
3. Wise DR, Thompson CB. Glutamine addiction: a new therapeutic target in cancer. Trends Biochem Sci 2010;35:427–33.
4. Hensley CT, Wasti AT, DeBerardinis RJ. Glutamine and cancer: cell biology, physiology, and clinical opportunities. J Clin Invest 2013;123:3678–84.
5. Gao P, Tchernyshyov I, Chang TC, Lee YS, Kita K, Ochi T, et al. c-Myc suppression of miR-23a/b enhances mitochondrial glutaminase expression and glutamine metabolism. Nature 2009;458:762–5.
6. Wang JB, Erickson JW, Fuji R, Ramachandran S, Gao P, Dinavahi R, et al. Targeting mitochondrial glutaminase activity inhibits oncogenic transformation. Cancer Cell 2010;18:207–19.
7. Seltzer MJ, Bennett BD, Joshi AD, Gao P, Thomas AG, Ferraris DV, et al. Inhibition of glutaminase preferentially slows growth of glioma cells with mutant IDH1. Cancer Res 2010;70:8981–7.
8. Cheng T, Sudderth J, Yang C, Mullen AR, Jin ES, Mates JM, et al. Pyruvate carboxylase is required for glutamine-independent growth of tumor cells. Proc Natl Acad Sci U S A 2011;108:8674–9.
9. Le A, Lane A, Hamaker M, Bose S, Gouw A, Barbi J, et al. Glucose-independent glutamine metabolism via TCA cycling for proliferation and survival in B cells. Cell Metabolism 2012;15:110–21.
10. van den Heuvel AP, Jing J, Wooster RF, Bachman KE. Analysis of glutamine dependency in non-small cell lung cancer: GLS1 splice variant GAC is essential for cancer cell growth. Cancer Biol Ther 2012;13:1185–94.
11. Yuneva MO, Fan TW, Allen TD, Higashi RM, Ferraris DV, Tsukamoto T, et al. The metabolic profile of tumors depends on both the responsible genetic lesion and tissue type. Cell Metab 2012;15:157–70.
12. Son J, Lyssiotis CA, Ying H, Wang X, Hua S, Ligorio M, et al. Glutamine supports pancreatic cancer growth through a KRAS-regulated metabolic pathway. Nature 2013;496:101–5.
13. Gameiro PA, Yang J, Metelo AM, Perez-Carro R, Baker R, Wang Z, et al. In vivo HIF-mediated reductive carboxylation is regulated by citrate levels and sensitizes VHL-deficient cells to glutamine deprivation. Cell Metab 2013;17:372–85.
14. Timmerman LA, Holton T, Yuneva M, Louie RJ, Padro M, Daemen A, et al. Glutamine sensitivity analysis identifies the xCT Antiporter as a common triple-negative breast tumor therapeutic target. Cancer Cell 2013;24:450–65.
15. Cassago A, Ferreira AP, Ferreira IM, Fornezari C, Gomes ER, Greene KS, et al. Mitochondrial localization and structure-based phosphate activation mechanism of glutaminase C with implications for cancer metabolism. Proc Natl Acad Sci U S A 2012;109:1092–7.
16. Kung HN, Marks JR, Chi JT. Glutamine synthetase is a genetic determinant of cell type-specific glutamine independence in breast epithelia. PLoS Genet 2011;7:e1002229.
17. Catane R, Von Hoff DD, Glaubiger DL, Muggia FM. Azaserine, DON, and azotomycin: three diazo analogs of L-glutamine with clinical antitumor activity. Cancer Treat Rep 1979;63:1033–8.
18. Robinson MM, McBryant SJ, Tsukamoto T, Rojas C, Ferraris DV, Hamilton SK, et al. Novel mechanism of inhibition of rat kidney-type glutaminase by bis-2-(5-phenylacetamido-1,2,4-thiadiazol-2-yl)ethyl sulfide (BPTES). Biochem J 2007;406:407–14.
19. Shukla K, Ferraris DV, Thomas AG, Stathis M, Duvall B, Delahanty G, et al. Design, synthesis, and pharmacological evaluation of bis-2-(5-phenylacetamido-1,2,4-thiadiazol-2-yl)ethyl sulfide 3 (BPTES) analogs as glutaminase inhibitors. J Med Chem 2012;55:10551–63.
20. Kisner DL, Catane R, Muggia FM. The rediscovery of DON (6-diazo-5-oxo-L-norleucine). Recent Results Cancer Res 1980;74:258–63.
21. Hartwick EW, Curthoys NP. BPTES inhibition of hGA(124–551), a truncated form of human kidney-type glutaminase. J Enzyme Inhib Med Chem 2012;27:861–7.
22. DeLaBarre B, Gross S, Fang C, Gao Y, Jha A, Jiang F, et al. Full-length human glutaminase in complex with an allosteric inhibitor. Biochemistry 2011;50:10764–70.
23. Thangavelu K, Pan C, Karlberg T, Balaji G, Uttamchandani M, Suresh V, et al. Structural basis for the allosteric inhibitory mechanism of human kidney-type glutaminase (KGA) and its regulation by Raf-Mek-Erk signaling in cancer cell metabolism. PNAS 2012;109:7705–10.
24. Qie S, Chu C, Li W, Wang C, Sang N. ErbB2 activation upregulates glutaminase 1 expression which promotes breast cancer cell proliferation. J Cell Biochem 2014;115:498–509.
25. Newcomb RW, inventor; Elan Pharmaceuticals I, assignee. Selective inhibition of glutaminase by bis-thiadiazoles. United States patent US 6451828. 2002 Sep 17.
26. Li J, Chen L, Goyal B, Laidig G, Stanton TF, Sjogren EB, inventors; Calithera Biosciences I, assignee. Heterocyclic inhibitors of glutaminase. United States patent US 8604016. 2013 Dec 10.
27. Neve RM, Chin K, Fridlyand J, Yeh J, Baehner FL, Fevr T, et al. A collection of breast cancer cell lines for the study of functionally distinct cancer subtypes. Cancer Cell 2006;10:515–27.
28. Krebs HA. Metabolism of amino-acids: the synthesis of glutamine from glutamic acid and ammonia, and the enzymic hydrolysis of glutamine in animal tissues. Biochem J 1935;29:1951–69.
29. Curthoys NP, Watford M. Regulation of glutaminase activity and glutamine metabolism. Annu Rev Nutr 1995;15:133–59.
30. Bannai S, Tateishi N. Role of membrane transport in metabolism and function of glutathione in mammals. J Membr Biol 1986;89:1–8.
31. Cancer Genome Atlas Network. Comprehensive molecular portraits of human breast tumours. Nature 2012;490:61–70.
32. Barretina J, Caponigro G, Stransky N, Venkatesan K, Margolin AA, Kim S, et al. The Cancer Cell Line Encyclopedia enables predictive modelling of anticancer drug sensitivity. Nature 2012;483:603–7.
33. Tanner M, Kapanen AI, Junttila T, Raheem O, Grenman S, Elo J, et al. Characterization of a novel cell line established from a patient with Herceptin-resistant breast cancer. Mol Cancer Ther 2004;3:1585–92.